Electronic Supplementary Information

Effects of Cationic Size on Thermoelectricity of PEDOT:PSS/Ionic Liquids Hybrid Films for Wearable Thermoelectric Generator Application

Kexing Jiang,[a]‡ *Shao-Huan Hong,*[a]‡ *Shih-Huang Tung*[b] *and Cheng-Liang Liu**[c]

[a] Department of Chemical and Materials Engineering, National Central University, Taoyuan 32001, Taiwan.

[b] Institute of Polymer Science and Engineering, National Taiwan University, Taipei 10617, Taiwan.

[c] Department of Materials Science and Engineering, National Taiwan University, Taipei 10617, Taiwan. E-mail: liucl@ntu.edu.tw

‡ These Authors Contributed equally to this work.

Characterization

The thicknesses of the thermoelectric films were measured by Alpha-Step® D-300 stylus profiler. The ultraviolet-visible-near-infrared (UV-Vis-NIR) absorption spectra were measured using a Hitachi U4100 spectrophotometer The Raman spectra of the films were obtained using a Raman spectroscopy (Horiba Jobin-Yvon LabRam HR800) with a Nd:YAG laser with the excitation wavelength of 532 nm. A surface chemical analysis instrument (VG Scientific ESCALAB 250) was employed to measure the X-ray photoelectron spectroscopy (XPS) spectra. Synchrotron-based GIXRD was performed at the B13A1 beamlines at National Synchrotron Radiation Research Center (NSRRC, Taiwan). Surface morphologies of the PEDOT:PSS films were determined by an tapping mode atomic force microscopy (Hitachi 5100N) under ambient condition. The work function was determined from the photoelectron emission yield measured by a Photon Electron Spectroscopy in Air (PESA) system (RIKEN KEIKI AC-2) operating at room temperature. The carrier concentration and mobility measurements were performed using a Hall measurement system (Ecopia HMS-3000) at room temperature.

Table S1 Summary of the thermoelectric properties of PEDOT:PSS/ionic liquids hybrid films.

Ionic liquid	Process	Conductivity [S cm^{-1}]	Seebeck coefficient [μV K^{-1}]	Power factor [μW m^{-1} K^{-2}]	Ref.
Li TFSI	Solution mixing	~1000	19-35	75	1
MMIM BF_4	Solution mixing	330.8	35.7	39.8	This work
MMIM TFSI	Solution mixing	520	17	15	2
EMIM BF_4	Solution mixing	497.2	32.7	53.1	This work
EMIM TFSI	Solution mixing	810	12	11	2
EMIM DCA	Solution mixing	275	35	33	3
EMIM DCA	Solution mixing	913	47	167	4
EMIM DCI	Solution mixing	538	29	42	3
EMIM TCM	Solution mixing	1000	30	90	5
EMIM TCM	Solution mixing	1163	38.8	175	6
EMIM TCM	Solution mixing	~140	~22		7
EMIM TCB	Solution mixing	~85	~23		7
EMIM TCB	Solution mixing	~600	18	28	4

EMIM ES	Solution mixing	~32	~25		7
BMIM BF_4	Solution mixing	566.3	31.6	56.7	This work
BMIM BF_4	Solution mixing	174.87	30.1	8.4	8
BMIM BF_4	Solution mixing	~570	25	29	4
BMIM Br	Solution mixing	123.07	30.6	9.9	8
HMIM BF_4	Solution mixing	729.0	28.7	60.1	This work
MMIM BF_4	Post treatment	1447.3	24.4	86.2	This work
BMIM TFSI	Post treatment	641	61.1	239.2	9
BMIM OTf	Post treatment	1260±61	34.8±1.8	152±11.2	10
BMIM BF_4	Post treatment	1654.2	19.6	63.5	This work
BMIM BF_4	Post treatment	1188±45	33.9±1.9	137±12.5	10
EMIM TCM	Post treatment	~1100	31.9	117	5
EMIM TFSI	Post treatment	380	42	40	11
EMIM DCA	Post treatment	450	42	85	4
EMIM DCA	Post treatment	568.2	38.4	83.8	12
EMIM DCA	Post treatment	3400	43		13
EMIM DCA	Post treatment	~1500-1600	~65	754	14
EMIM TCB	Post treatment	330	25	25	4

EMIM BF_4	Post treatment	1534.1	21.4	70.3	This work
EMIM BF_4	Post treatment	480	27	40	4
EMIM BF_4	Post treatment	~700	~24	38.46	15
HMIM BF_4	Post treatment	1974.2	19.5	75.1	This work
$[CoCl_2 \cdot 6H_2O]$:[ChCl]	Post treatment	1648±56	21.6±0.4	76.8	16

Table S2 Physical properties of ionic liquids in this study.

Ionic liquid	Viscosity [mPa s]	Density [g cm^{-3}]	Molar mass [g mol^{-1}]
MMIM BF_4	34	1.30	183.95
EMIM BF_4	60	1.29	197.97
BMIM BF_4	140	1.26	226.05
HMIM BF_4	260	1.15	268.10

Table S3 XPS Results: deconvoluted S 2p peaks of the XPS spectra for spin-coated pristine PEDOT:PSS film and PEDOT:PSS/XMIM BF_4 hybrid films with formamide post treatment.

Sample	Chemical state	Binding energy [eV]	Area percentage [%]	PEDOT to PSS composition ratio
PEDOT:PSS	PSS S $2p_{1/2}$	169.39	23.67	1:2.44
	PSS S $2p_{3/2}$	168.23	47.30	
	PEDOT S $2p_{1/2}$	165.47	19.35	
	PEDOT S $2p_{3/2}$	164.31	9.68	
PEDOT:PSS /MMIM BF_4	PSS S $2p_{1/2}$	168.84	17.94	1:1.16
	PSS S $2p_{3/2}$	167.68	35.85	
	PEDOT S $2p_{1/2}$	165.41	15.41	
	PEDOT S $2p_{3/2}$	164.25	30.80	
PEDOT:PSS /EMIM BF_4	PSS S $2p_{1/2}$	169.01	18.40	1:1.23
	PSS S $2p_{3/2}$	167.85	36.77	
	PEDOT S $2p_{1/2}$	165.45	14.95	

	PEDOT S $2p_{3/2}$	164.29	29.89	
PEDOT:PSS /BMIM BF_4	PSS S $2p_{1/2}$	168.95	18.60	1:1.26
	PSS S $2p_{3/2}$	167.79	37.18	
	PEDOT S $2p_{1/2}$	165.49	14.75	
	PEDOT S $2p_{3/2}$	164.33	29.48	
PEDOT:PSS /HMIM BF_4	PSS S $2p_{1/2}$	169.16	19.14	1:1.35
	PSS S $2p_{3/2}$	168.00	38.26	
	PEDOT S $2p_{1/2}$	165.51	14.21	
	PEDOT S $2p_{3/2}$	164.35	28.39	

Table S4 Summary of the thermoelectric properties of PEDOT:PSS-based thermoelectric generators.

Treatment	Conductivity [S cm^{-1}]	Seebeck coefficient [μV K^{-1}]	Power factor [μW m^{-1} K^{-2}]	Leg numbers	Output voltage [mV]	Output power [nW]	Ref.
PEDOT:PSS/MMIM BF_4	1447.3	24.4	86.2	7	2.4	16.5 (μW cm^{-2})	This work
Doping with BSA and DMSO/HZ	1119	42.6	203.1	16	4.6		17
PEDOT:PSS (Clevios PJET 700) ink printing	17±1.5	600±70	17.12±4.6	4/4	29.36	0.419	18
Spray Printing and PS treatment	~600	~15		74	9.21	2.23	19
Sulfuric acid treatment	2500	20.6	107	5	2		20
Formamide, Sulfuric acid and $NaBH_4$ treatment	1786	28.1	141	14	2.9		21
Polymerized PEDOT:OTf	2215±665	18.0	105	312		16.5±0.5 (nW K^{-2} m^{-2})	22
Treated with EG/$NaHCO_3$	770	48	183	4/4	6.98	98 (μW cm^{-2})	23
PEDOT:PSS/WPU fibers	730	~19	26.1	5/5		0.311	24
PEDOT:PSS/WPU/EMIM TCM	~140	~22		10	6.5	~25	7
EG, DMSO and BMIM BF_4 treatment	172.5	14.8	4.77	5/5	20.7	481.2 (μW cm^{-2})	25

$^{Ag@}NC_{Dots}$/PEDOT:PSS/PVA	287.4±19	65.55±3	123.5±6	12	15.12	15.59	26
EG-H_2SO_4 treatment	676.59	13.13	9.42		1.7		27
PEDOT:PSS/Te nanorod composite	122.4	51.6	51.4	8	2.5		28

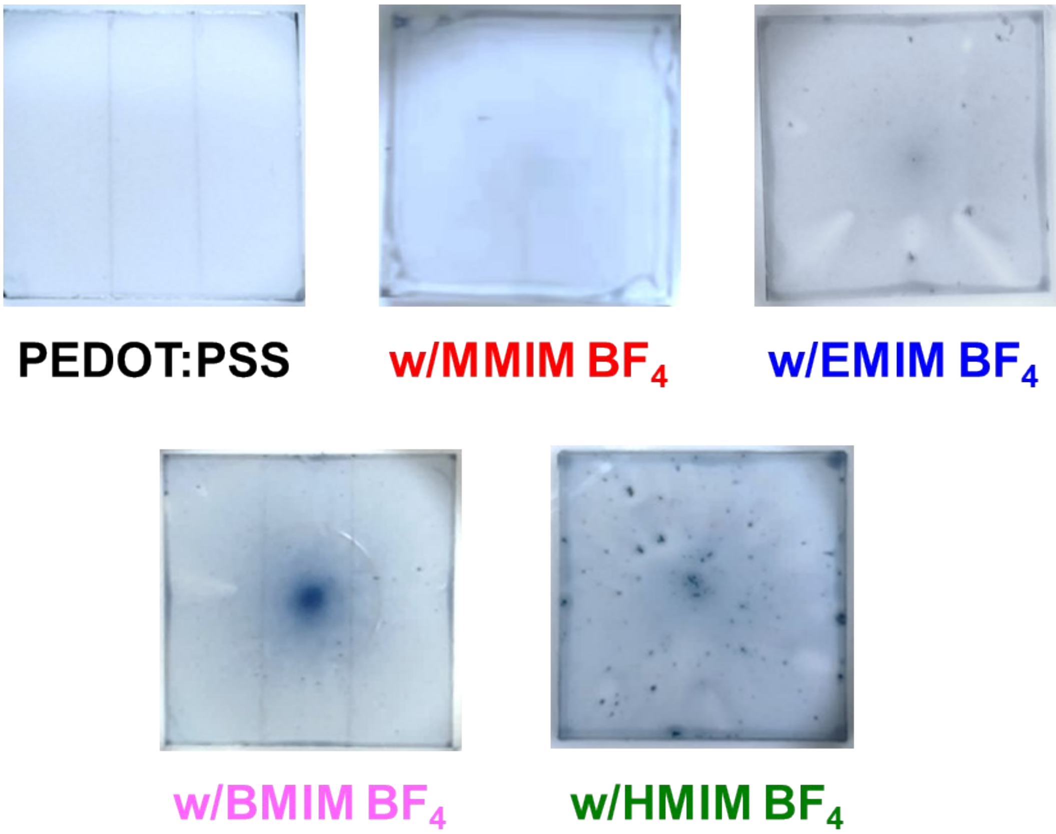

Fig. S1 Photograph of spin-coated XMIM BF_4 modified PEDOT:PSS films.

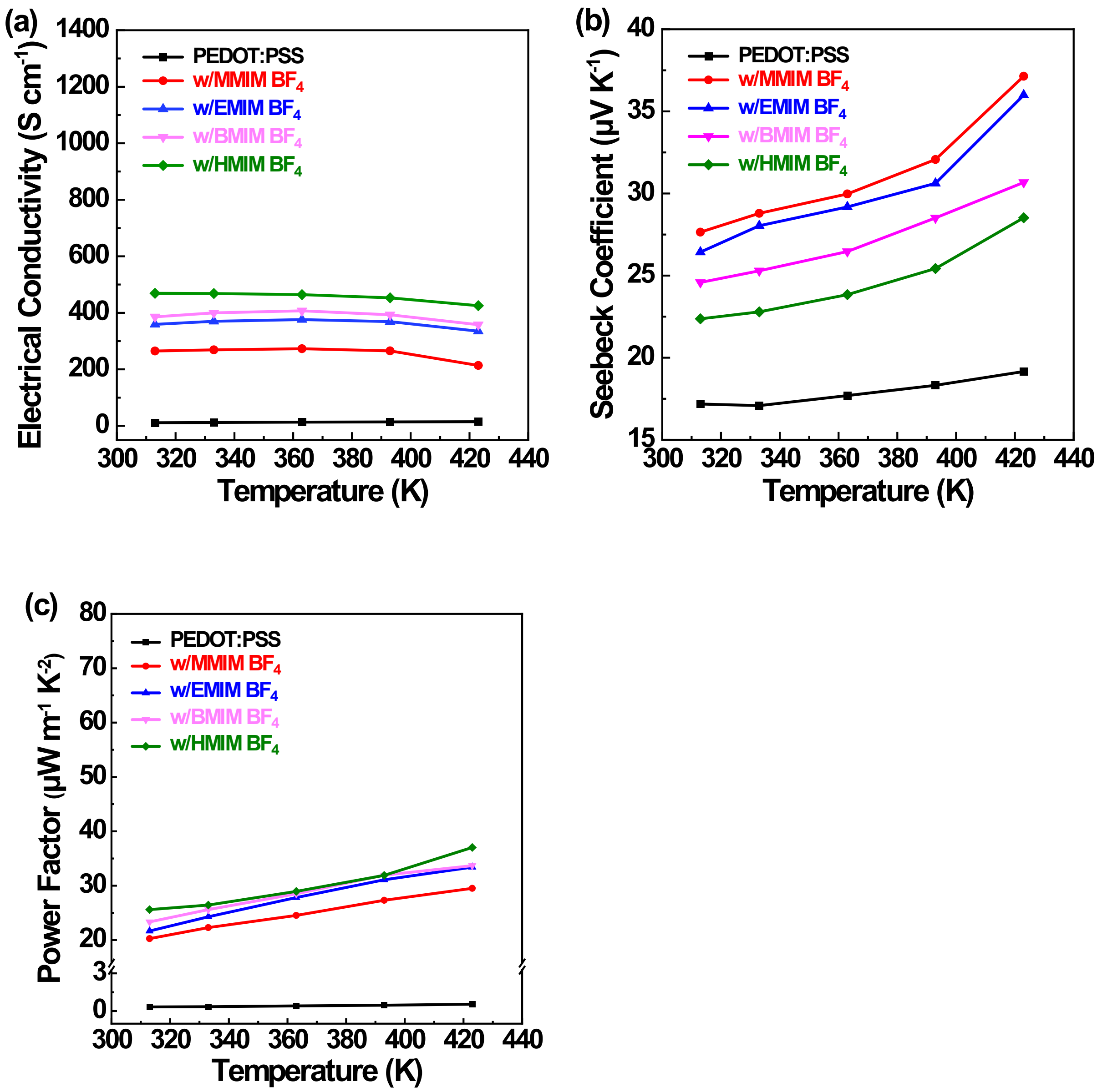

Fig. S2 Temperature-dependent (a) electrical conductivity, (b) Seebeck coefficient, and (c) power factor of the spin-coated pristine PEDOT:PSS and PEDOT:PSS/XMIM BF_4 (1%) hybrid films without DMSO post-treatment. It is noted that the PEDOT:PSS mixed with MMIM BF_4, EMIM BF_4, BMIM BF_4, HMIM BF_4 is denoted as w/MMIM BF_4, w/EMIM BF_4, w/BMIM BF_4, w/HMIM BF_4 respectively.

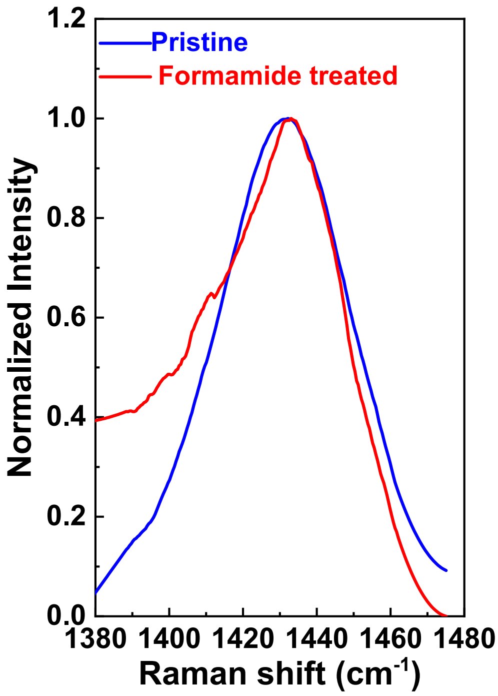

Fig. S3 Raman spectra of spin-coated pristine PEDOT:PSS films and one with formamide post-treatment.

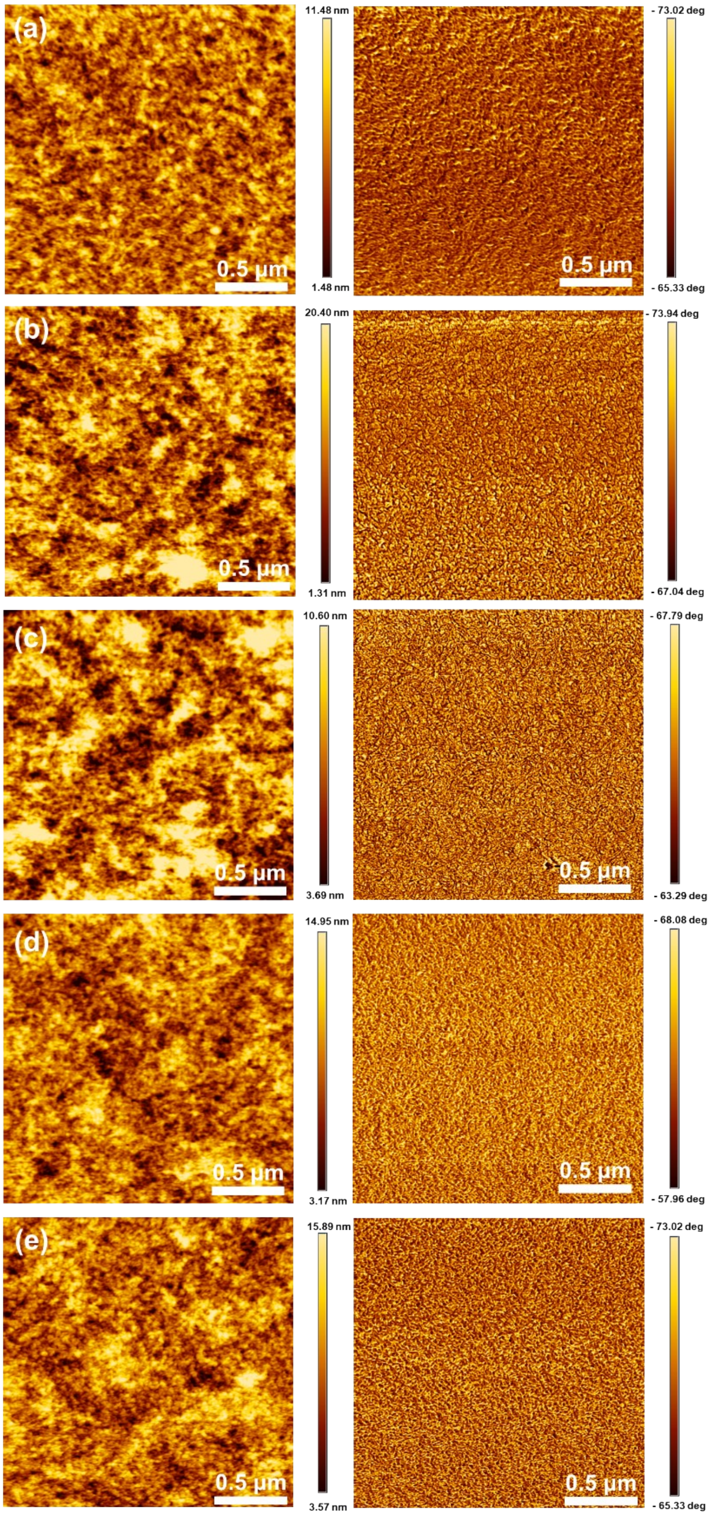

Fig. S4 AFM height (left) and phase (right) images of spin-coated (a) pristine PEDOT:PSS films and (b) PEDOT:PSS/MMIM BF_4, (c) PEDOT:PSS/EMIM BF_4, (d) PEDOT:PSS/BMIM BF_4, (e) PEDOT:PSS/HMIM BF_4 hybrid films with formamide post treatment.

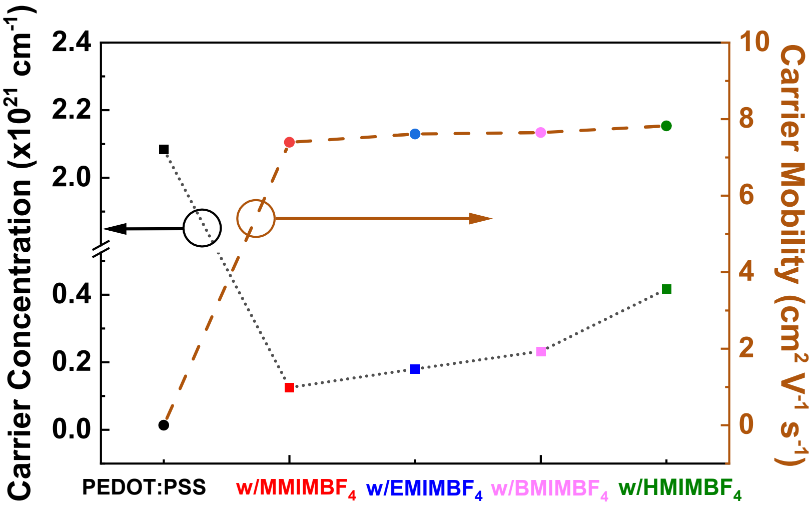

Fig. S5 Hall effect measurement of carrier concentration and mobility of spin-coated pristine PEDOT:PSS and PEDOT:PSS/XMIM BF_4 hybrid films with formamide post treatment.

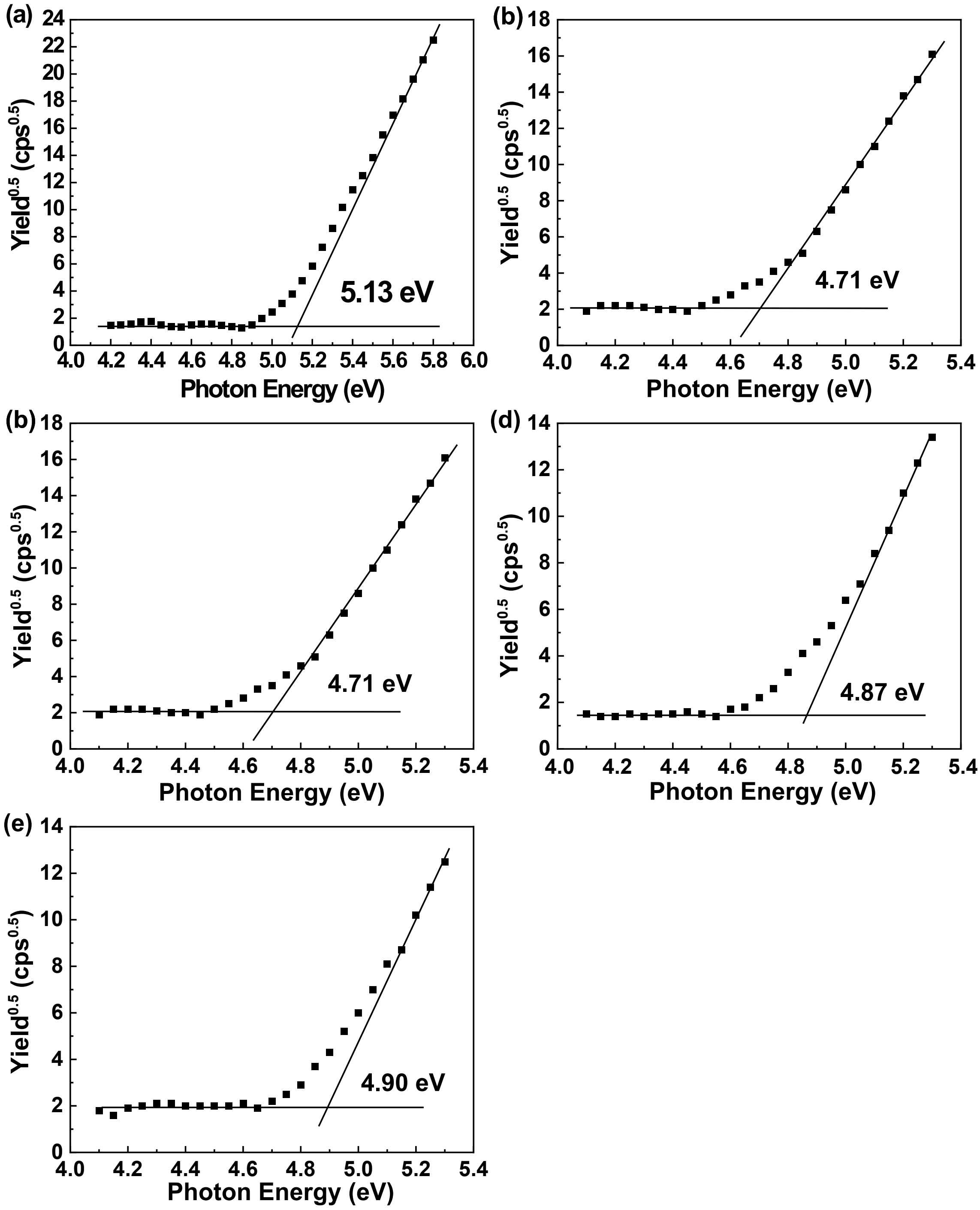

Fig. S6 Photoelectron spectroscopy in air (PESA) measurement of spin-coated (a) pristine PEDOT:PSS films and (b) PEDOT:PSS/MMIM BF_4, (c) PEDOT:PSS/EMIM BF_4, (d) PEDOT:PSS/BMIM BF_4, (e) PEDOT:PSS/HMIM BF_4 hybrid films with formamide post treatment.

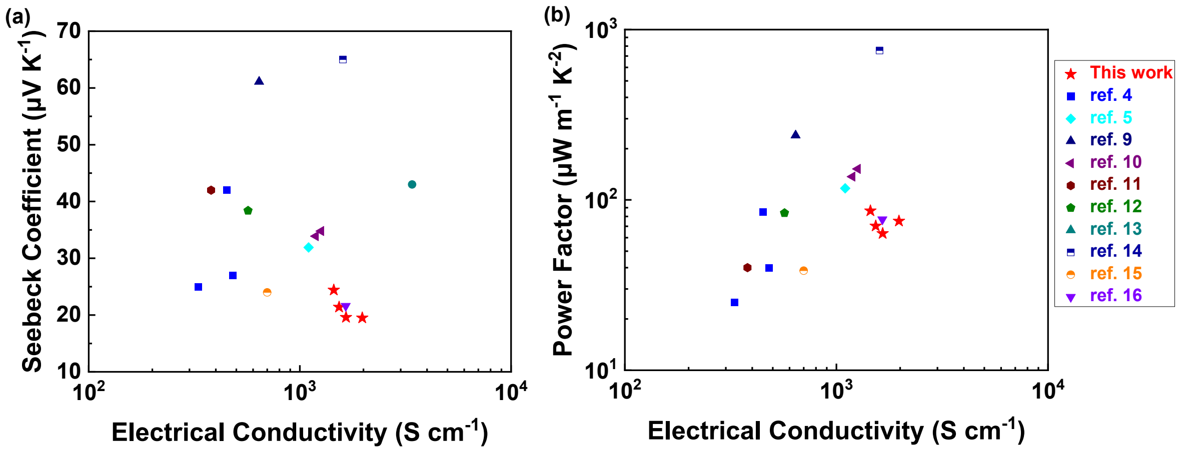

Fig. S7 (a) Seebeck coefficient and (b) power factor vs. electrical conductivity for previously reported PEDOT:PSS films post-treated ionic liquids and this work.

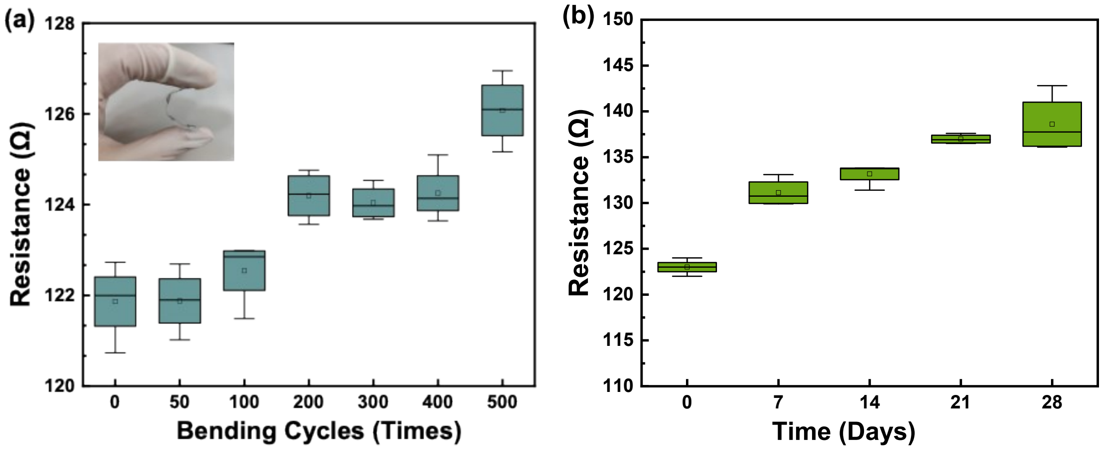

Fig. S8 Relative resistance of the flexible thermoelectric generators versus (a) the bending cycles at bending radius of 3 mm (The inset shows photo of assembled thermoelectric generator supported by PET and demonstrates good flexibility) and (b) time under the ambient condition (relative humidity of ~ 40%, room temperature).

Reference

1. Q. K. Li, M. J. Deng, S. M. Zhang, D. K. Zhao, Q. L. Jiang, C. F. Guo, Q. Zhou and W. S. Liu, *J. Mater. Chem. C*, 2019, **7**, 4374-4381.
2. A. Mazaheripour, S. Majumdar, D. Hanemann-Rawlings, E. M. Thomas, C. McGuiness, L. d'Alencon, M. L. Chabinyc and R. A. Segalman, *Chem. Mater.*, 2018, **30**, 4816-4822.
3. S. Kee, H. Kim, S. H. K. Paleti, A. El Labban, M. Neophytou, A.-H. Emwas, H. N. Alshareef and D. Baran, *Chem. Mater.*, 2019, **31**, 3519-3526.
4. N. Saxena, B. Pretzl, X. Lamprecht, L. Bießmann, D. Yang, N. Li, C. Bilko, S. Bernstorff and P. Müller-Buschbaum, *ACS Appl. Mater. Interfaces*, 2019, **11**, 8060-8071.
5. Q. Li, Q. Zhou, L. Wen and W. Liu, *J. Materiomics*, 2020, **6**, 119-127.
6. X. Li, R. Zou, Z. Liu, J. Mata, B. Storer, Y. Chen, W. Qi, Z. Zhou and P. Zhang, *npj Flex. Electron.*, 2022, **6**, 6.
7. N. Kim, S. Lienemann, I. Petsagkourakis, D. A. Mengistie, S. Kee, T. Ederth, V. Gueskine, P. Leclere, R. Lazzaroni, X. Crispin and K. Tybrandt, *Nat. Commun.*, 2020, **11**, 1424.
8. C. Liu, J. Xu, B. Lu, R. Yue and F. Kong, *J. Electron. Mater.*, 2012, **41**, 639-645.
9. T. A. Yemata, Y. Zheng, A. K. K. Kyaw, X. Wang, J. Song, W. S. Chin and J. Xu, *Front. Chem.*, 2020, **7**, 870.
10. T. A. Yemata, Y. Zheng, A. K. K. Kyaw, X. Z. Wang, J. Song, W. S. Chin and J. W. Xu, *Mater. Adv.*, 2020, **1**, 3233-3242.
11. J. Atoyo, M. R. Burton, J. McGettrick and M. J. Carnie, *Polymers*, 2020, **12**, 559.
12. M. Z. Du, X. Y. Chen and K. Zhang, *ACS Appl. Energy Mater.*, 2021, **4**, 4070-4080.
13. H. Cheng and J. Ouyang, *Adv. Energy Mater.*, 2020, **10**, 2001633.
14. Z. Fan, D. Du, X. Guan and J. Ouyang, *Nano Energy*, 2018, **51**, 481-488.
15. J. J. Luo, D. Billep, T. Waechtler, T. Otto, M. Toader, O. Gordan, E. Sheremet, J. Martin, M. Hietschold, D. R. T. Zahnd and T. Gessner, *J. Mater. Chem. A*, 2013, **1**, 7576-7583.
16. Y. N. Lu, A. Y. Wu, C. W. Sha, X. C. Hang and D. J. Young, *Chem Asian J.*, 2021, **16**, 2740-2744.
17. C. Wang, K. Sun, J. Fu, R. Chen, M. Li, Z. Zang, X. Liu, B. Li, H. Gong and J. Ouyang, *Adv. Sustainable Syst.*, 2018, **2**, 1800085.

18. S. Ferhat, C. Domain, J. Vidal, D. Noël, B. Ratier and B. Lucas, *Sustainable Energy Fuels*, 2018, **2**, 199-208.
19. S. Hwang, I. Jeong, J. Park, J.-K. Kim, H. Kim, T. Lee, J. Kwak and S. Chung, *ACS Appl. Mater. Interfaces*, 2020, **12**, 26250-26257.
20. Z. Li, H. Sun, C.-L. Hsiao, Y. Yao, Y. Xiao, M. Shahi, Y. Jin, A. Cruce, X. Liu, Y. Jiang, W. Meng, F. Qin, T. Ederth, S. Fabiano, W. M. Chen, X. Lu, J. Birch, J. W. Brill, Y. Zhou, X. Crispin and F. Zhang, *Adv. Electron. Mater.*, 2018, **4**, 1700496.
21. S. Xu, M. Hong, X.-L. Shi, Y. Wang, L. Ge, Y. Bai, L. Wang, M. Dargusch, J. Zou and Z.-G. Chen, *Chem. Mater.*, 2019, **31**, 5238-5244.
22. E. Yvenou, M. Sandroni, A. Carella, M. N. Gueye, J. Faure-Vincent, S. Pouget, R. Demadrille and J.-P. Simonato, *Mater. Chem. Front.*, 2020, **4**, 2054-2063.
23. I. Paulraj, T.-F. Liang, T.-S. Yang, C.-H. Wang, J.-L. Chen, Y. W. Wang and C.-J. Liu, *ACS Appl. Mater. Interfaces*, 2021, **13**, 42977-42990.
24. N. Wen, Z. Fan, S. Yang, Y. Zhao, C. Li, T. Cong, H. Huang, J. Zhang, X. Guan and L. Pan, *Chem. Eng. J.*, 2021, **426**, 130816.
25. J. Liu, Y. Jia, Q. Jiang, F. Jiang, C. Li, X. Wang, P. Liu, P. Liu, F. Hu, Y. Du and J. Xu, *ACS Appl. Mater. Interfaces*, 2018, **10**, 44033-44040.
26. A. F. Al Naim, S. S. Ibrahim and A. g. El-Shamy, *Polymer*, 2021, **226**, 123792.
27. Y. Pan, Y. Song, Q. Jiang, Y. Jia, P. Liu, H. Song and G. Liu, *Synth. Met.*, 2022, **283**, 116969.
28. H. Song and K. Cai, *Energy*, 2017, **125**, 519-525.